

# Far-Infrared Spectroscopy of the Poly(ethylene oxide)<sub>x</sub>–LiCF<sub>3</sub>SO<sub>3</sub> System

Varuni Seneviratne,<sup>†</sup> J. E. Furneaux,<sup>†</sup> and Roger Frech<sup>\*,‡</sup>

Department of Physics and Astronomy and Department of Chemistry and Biochemistry, University of Oklahoma, Norman, Oklahoma 73019

Received December 3, 2001; Revised Manuscript Received May 21, 2002

**ABSTRACT:** The infrared absorption spectrum of poly(ethylene oxide)–LiCF<sub>3</sub>SO<sub>3</sub> yields two broad, distinct Li–O stretching bands (“cage” modes) between 395 and 440 cm<sup>−1</sup>. An analysis of the integrated band intensities as a function of salt concentration demonstrates that each mode originates in the motion of all lithium ions in all potential energy environments, rather than each band being due to a distinct ionic species. Multiple band structure is observed in several low-frequency, intramolecular CF<sub>3</sub>SO<sub>3</sub><sup>−</sup> modes. These data are compared with the extensively studied CF<sub>3</sub> symmetric deformation mode in order to identify the ionic species associated with each band component.

## 1. Introduction

The solvation of salts in high molecular weight polymers such as poly(ethylene oxide), PEO, results in polymer electrolytes with significant ionic conductivity.<sup>1</sup> Consequently, lithium ion-conducting polymers are now being developed for use in lithium rechargeable batteries.<sup>2,3</sup> However, the ionic conductivity of these materials must be improved before successful commercialization can occur. Thus, there is a high level of interest in understanding fundamental factors that control ionic conductivity in order to facilitate this improvement. There is evidence that conductivity occurs predominantly in the amorphous phase of polymer electrolytes,<sup>4</sup> with cation–anion interactions, cation–polymer interactions,<sup>5</sup> and polymer segmental motion<sup>6</sup> all playing roles in the transport mechanism.

Vibrational spectroscopy is a particularly useful probe of PEO–salt systems and therefore has been used widely to study them. For instance, intramolecular modes of polyatomic anions provide useful information about cation–anion interactions,<sup>7–9</sup> and the backbone CH<sub>2</sub> rocking modes yield information about changes in the local structure of the polymer backbone due to the coordination of the cation by PEO ether oxygen atoms.<sup>10,11</sup> Technologically, the conductivity of the cations is most important, and the interaction of these cations with their environment is of primary interest. PEO and anionic modes are all relatively indirect measures of the cationic environment. The only direct infrared spectroscopic signature of this environment is the set of modes associated with the motion of the cation in a “cage” defined by the coordinating oxygen atoms of both the polyether and the anions. Papke et al. first observed these vibrational modes in PEO containing Na, K, Rb, and Cs salts in 1981.<sup>7</sup> A systematic study of this mode in lithium-containing PEO-based electrolytes has not been reported. Therefore, investigating the spectral behavior of these modes in a series of P(EO)<sub>x</sub>LiCF<sub>3</sub>SO<sub>3</sub> compositions is a major goal of this work.

This system of cationic modes is placed in perspective by concurrent studies of anionic modes. The CF<sub>3</sub>SO<sub>3</sub><sup>−</sup>

(triflate, abbreviated Tf) anion is selected because the frequencies of several anionic intramolecular modes are sensitive to cation–anion interactions that produce different anionic species such as “free” ions, contact ion pairs, and more highly associated aggregates. The resulting bands are well-separated in frequency and allow unambiguous identification of the various ionic species. Early vibrational studies emphasized the SO<sub>3</sub> symmetric stretch mode,  $\nu_s(\text{SO}_3)$ ,<sup>8,12</sup> and later the CF<sub>3</sub> symmetric deformation mode,  $\delta_s(\text{CF}_3)$ .<sup>13,14</sup> Here we use the  $\delta_s(\text{CF}_3)$  mode as a source of baseline information to study the cationic modes. Studying other intramolecular triflate modes using  $\delta_s(\text{CF}_3)$  baseline data provides further insight into the nature of the cationic environment and the nature of cation–anion interactions. Such insight is another goal of this paper.

## 2. Experimental Section

Lithium triflate, LiTf (Aldrich, 96%), was dried for 24 h at 10<sup>−2</sup> mbar and 110 °C, allowed to cool to room temperature, and stored in a drybox in a nitrogen atmosphere. We also obtained PEO with an average molecular weight of 100 000 Da from Aldrich and vacuum-dried it at 50 °C before cooling to room temperature. We used acetonitrile as received (Fisher Biotech) for the low molecular weight solvent in this study.

Measured amounts of PEO and LiTf were stirred in acetonitrile for not less than 24 h at room temperature to make solutions characterized by their ether oxygen to cation atomic ratios (EO:Li). The resulting viscous solutions were then cast as thin films on Teflon plates. The films were cured for at least 24 h to produce solvent-free films. The entire sample preparation was carried out in a drybox filled with nitrogen.

We recorded infrared transmission spectra of free-standing films from 50 to 4000 cm<sup>−1</sup> on a Bruker IFS66V Fourier transform infrared (FTIR) spectrometer at a spectral resolution of 1 cm<sup>−1</sup>. We used a Mylar beam splitter and a DTGS detector with a polyethylene window for the spectral region from 50 to 700 cm<sup>−1</sup> and switched to a KBr beam splitter for the region from 400 to 4000 cm<sup>−1</sup>. We then performed curve-fitting analyses of the resulting spectra using Galactic Grams software, version 5.05. Overlapping data in the spectral range from 400 to 700 cm<sup>−1</sup> were used to ensure consistent comparisons of spectral intensities recorded with different beam splitters.

## 3. Results and Discussion

**3.1. The Li–O Stretching Modes.** We present room temperature infrared spectra from 500 to 360 cm<sup>−1</sup> in

<sup>†</sup> Department of Physics and Astronomy.

<sup>‡</sup> Department of Chemistry and Biochemistry.

**Table 1. Relative Integrated Intensities of Triflate  $\delta_s(\text{CF}_3)$  Bands Assigned to "Free" Ions, Contact Ion Pairs, and the Aggregate  $[\text{Li}_2\text{Tf}]^+$  Species and the Two  $\nu(\text{Li-O})$  Modes<sup>a</sup>**

assignment	composition EO:Li					
	80:1	60:1	40:1	20:1	10:1	5:1
"free" ions (753 cm <sup>-1</sup> )	27	11	14	4	2	5
ion pairs (757 cm <sup>-1</sup> )	48	25	27	19	10	13
triple ions (761 cm <sup>-1</sup> )	25	64	59	77	88	82
$\nu_1(\text{Li-O})$	85 (464 cm <sup>-1</sup> )	85 (462 cm <sup>-1</sup> )	83 (460 cm <sup>-1</sup> )	87 (447 cm <sup>-1</sup> )	88 (440 cm <sup>-1</sup> )	84 (439 cm <sup>-1</sup> )
$\nu_2(\text{Li-O})$	15 (401 cm <sup>-1</sup> )	15 (408 cm <sup>-1</sup> )	17 (403 cm <sup>-1</sup> )	13 (395 cm <sup>-1</sup> )	12 (393 cm <sup>-1</sup> )	16 (391 cm <sup>-1</sup> )

<sup>a</sup> The frequency of each band, in cm<sup>-1</sup>, is given in parentheses.

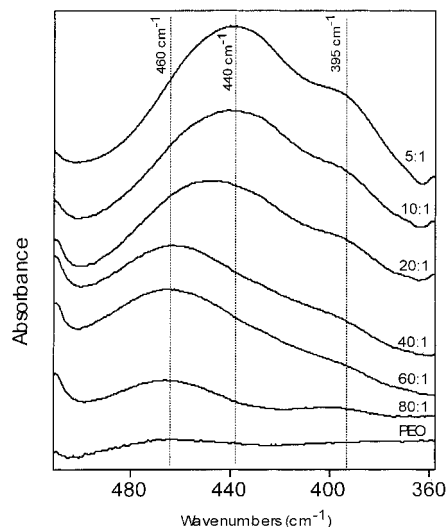


**Figure 1.** IR spectra of PEO and P(EO)<sub>n</sub>LiCF<sub>3</sub>SO<sub>3</sub> complexes ( $n = 80, 60, 40, 20, 10, 5$ ) in the  $\nu(\text{Li-O})$  region. The intensity of the 5:1 spectrum has been reduced to fit the figure.

Figure 1. In pure PEO there is a weak, broad feature between 480 and 450 cm<sup>-1</sup>. At low salt concentrations from 80:1 to 40:1, a broad feature centered at roughly 460 cm<sup>-1</sup> grows in intensity. At a slightly higher concentration, 20:1, this feature is masked by a broad band centered at roughly 450 cm<sup>-1</sup>. At the higher concentrations of 10:1 and 5:1, this band is centered at 440 cm<sup>-1</sup>. We also see a low-frequency shoulder at about 395 cm<sup>-1</sup> for all salt concentrations. The higher frequency band shifts gradually from 460 to 440 cm<sup>-1</sup> as the concentration increases from 80:1 to 5:1. We see a slight shift to lower frequencies in the 395 cm<sup>-1</sup> component as the salt concentration is increased from 80:1 to 60:1. Both of these features increase in intensity with further increase in salt concentration and dominate this spectral region in the 5:1 composition. We attribute these spectral features to the Li-O stretching or "cage" motion in accordance with assignments proposed by Papke et al. in 1982.<sup>15</sup> We designate the band centered between 440 and 460 cm<sup>-1</sup> as  $\nu_1(\text{Li-O})$  and the band at 395 cm<sup>-1</sup> as  $\nu_2(\text{Li-O})$ . We fit the features in this spectral region with two Gaussian bands and summarize the results in Table 1 and Figure 2. The thick lines (filled rectangles and circles) of Figure 2 represent the relative integrated intensities of two  $\nu(\text{Li-O})$  modes, while thin lines (open triangles, rectangles, and circles) represent relative integrated intensities of the various ionic species as determined from a curve-fitting analysis of the  $\delta_s(\text{CF}_3)$  spectral region. In Figure 1, we see qualitatively that the intensities of both  $\nu(\text{Li-O})$  modes grow together; i.e., the ratio of their areas is similar for all salt concentrations. Indeed, our curve-fitting parameters are

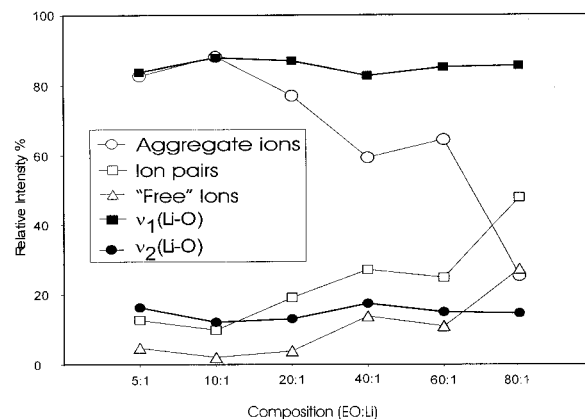


**Figure 2.** Relative integrated intensities of triflate  $\delta_s(\text{CF}_3)$  bands assigned to "free" ions, contact ion pairs, and the aggregate  $[\text{Li}_2\text{Tf}]^+$  species plotted as a function of composition expressed as EO:Li. Also shown are the relative intensities of the two  $\nu(\text{Li-O})$  modes.

consistent with a constant ratio as seen in Figure 2 and Table 1.

We now examine the origin of the two  $\nu(\text{Li-O})$  components. There are at least three explanations for these data:

1. Two absorption bands, each uniquely associated with lithium ions in a spectroscopically distinct cationic environment. (We note that there may be a number of different cation environments that result in two spectroscopically distinct cation environments.)
2. Two absorption bands resulting from a single asymmetric cationic environment. (Here the selection rules for a cation vibrating in such an environment predict three modes; two are then assumed to be spectroscopically indistinguishable.)
3. Two different absorption bands originating in all cations participating in a lithium-oxygen stretching motion regardless of potential energy environment.

The room temperature composition of a sample of P(EO)-LiTf is heterogeneous. The phase diagram<sup>16,17</sup> predicts a crystalline P(EO)<sub>3</sub>LiTf phase (referred to in this paper as the 3:1 compound) and a crystalline PEO phase. A number of studies also show the existence of an amorphous phase containing dissolved salt present as both "free" ions and Li<sup>+</sup>Tf<sup>-</sup> contact ion pairs. The triflate ion in P(EO)<sub>3</sub>LiTf has been shown to vibrate as the  $(\text{Li}_2\text{Tf})^+$  species.<sup>18,19</sup> Therefore, one possible explanation for the two Li-O components is that they originate from lithium ions in two different coordination environments, e.g., one band from Li<sup>+</sup> vibrating in a  $(\text{Li}_2\text{Tf})^+$  species and the other band from Li<sup>+</sup> vibrating in a Li<sup>+</sup>Tf<sup>-</sup> contact ion pair. To test this hypothesis, the relative concentrations of the various ionic species present can be estimated from the integrated band intensities of intramolecular triflate ion modes whose

frequencies are sensitive to ionic association. This calculation has been performed for the  $\delta_s(\text{CF}_3)$  mode, and the data are also summarized in Table 1 and Figure 2. We note that the percentages of integrated band intensities of the two Li–O stretching band components are relatively constant across the entire composition range from 80:1 to 5:1. Because the separate integrated intensities of the two  $\nu(\text{Li–O})$  modes are not correlated with the intensities of the  $\delta_s(\text{CF}_3)$  modes associated with different triflate ion (and hence lithium ion) environments, we conclude that the two components of the Li–O stretching mode do not originate in lithium ions vibrating in contact ion pairs and  $(\text{Li}_2\text{Tf})^+$  triple ions.

The above argument is further supported by the qualitative behavior of the bands. We clearly observe in Figure 1 that the high-frequency band is dominant throughout the concentration range. If these two modes were due to two different cationic environments, we would expect to see one band dominant at lower salt concentrations when ion pairs dominate and the other band dominant at higher salt concentrations in which the  $(\text{Li}_2\text{Tf})^+$  species is the major species.

The second hypothesis is that the intensities of the two  $\nu(\text{Li–O})$  bands primarily originate in domains of a distinct, well-defined yet asymmetric potential energy environment. The above requirement is most readily satisfied by the  $\text{P}(\text{EO})_3\text{LiTf}$  compound. In the compound, the lithium ion is 5-fold coordinated by three adjacent ether oxygen atoms from the PEO backbone and two triflate oxygen atoms (one from each of two triflate ions).<sup>20</sup> Consequently, the Li–O stretching vibrations are cage modes in which the  $\text{Li}^+$  undergoes translational motion in a potential energy environment defined by the five coordinating oxygen atoms. A free lithium ion has three translation degrees of freedom, which, in the solid state, become three independent lithium–oxygen vibrations. There are four lithium ions in the monoclinic cell of the compound, and an analysis of the lithium ion translational modes employing standard group theoretical methods demonstrates that the translatory vibrational motions can be classified under the irreducible representations of the unit cell group (isomorphous with the  $C_{2h}$  point group) according to  $\Gamma(\text{Li–O}) = 3A_g + 3B_g + 3A_u + 3B_u$ .

The simplicity of the spectrum argues that the Li–O stretching vibrations are highly decoupled in the compound and can be viewed as localized modes. On those grounds, we expect three components. The observation of only two distinct components suggests that, under this hypothesis, two of the modes have frequencies so similar that they cannot be spectrally resolved.

The third hypothesis is that the two absorption bands arise from all lithium ions participating in a lithium–oxygen stretching motion. To test this hypothesis, in Figure 3 we plot the total integrated intensity of the  $\nu(\text{Li–O})$  spectral region against the total integrated intensity of the  $\delta_s(\text{CF}_3)$  region. Our rationale for doing this is the following. Although the three distinct bands in the  $\delta_s(\text{CF}_3)$  region are attributed to “free” ions, contact ion pairs, and the  $(\text{Li}_2\text{Tf})^+$  species, there may be other ionic species present. For example, we cannot distinguish between truly free  $\text{Tf}^-$  ions and solvent-separated ion pairs. We are also unable to distinguish between  $\text{Li}^+\text{Tf}^-$  contact ion pairs and the triple anion species  $(\text{LiTf}_2)^-$ . Choosing to examine the dependence of the total  $\nu(\text{Li–O})$  integrated intensity with the total  $\delta_s(\text{CF}_3)$  integrated intensity is equivalent to examining the

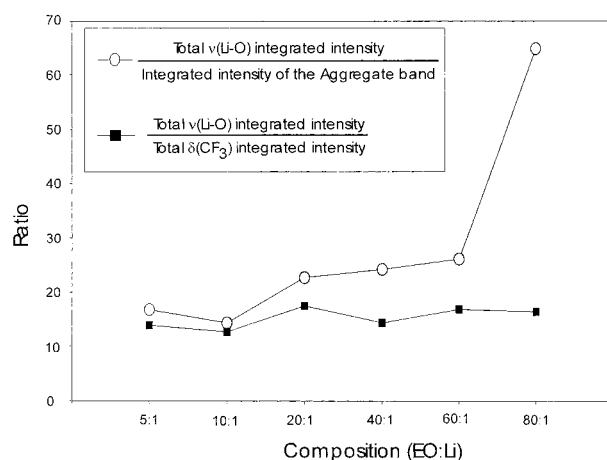


**Figure 3.** Ratios of total  $\nu(\text{Li–O})$  integrated intensity/integrated intensity of aggregate band and total  $\nu(\text{Li–O})$  integrated intensity/total integrated intensity of the  $\delta(\text{CF}_3)$  mode plotted as functions of composition expressed as EO:Li.

dependence on the total anion concentration, regardless of phase and ionic species present. In turn, because overall charge neutrality is required, this procedure is equivalent to examining the dependence of the total  $\nu(\text{Li–O})$  integrated intensity on the total cation concentration, regardless of phase and ionic speciation. It is evident from the figure that the plot (total  $\nu(\text{Li–O})$  integrated intensity/total  $\delta_s(\text{CF}_3)$  integrated intensity plotted against system composition) is constant over the entire composition range. Thus, hypothesis 3 provides the most consistent explanation of all data at all system compositions. Figure 3 also shows the ratio of the total  $\nu(\text{Li–O})$  integrated intensity to the integrated intensity of the  $(\text{Li}_2\text{Tf})^+$  band plotted against system composition. The deviation of the plot from a constant argues against hypothesis 2.

**3.2. Triflate Ion Intramolecular Modes.** Our next goal is to identify the bands due to ionic association in the anion modes, such as the  $\text{SO}_3$  symmetric deformation,  $\delta_s(\text{SO}_3)$ , the  $\text{SO}_3$  antisymmetric deformation,  $\delta_{as}(\text{SO}_3)$ , and the  $\text{CF}_3$  antisymmetric deformation,  $\delta_{as}(\text{CF}_3)$ . This is not an easy task, because some of the modes are degenerate in the isolated  $\text{Tf}^-$  ion. In some regions, there are overlapping PEO bands and possibly triflate overtone and combination bands. To overcome these problems, we prepared a 60:1 PEO:tetrabutylammonium triflate (TbTf) sample and measured its IR spectrum. The cation of this salt is quite bulky and does not form ion pairs or aggregates.<sup>21</sup> Therefore, in the PEO:TbTf spectrum, we see only triflate bands due to “free” ions. This information helps us to assign unambiguously the “free” triflate ion modes in the less well-characterized regions of the spectrum.

Bands identified as  $\delta_s(\text{SO}_3)$  are shown in Figure 4. At an 80:1 composition, there is a broad, asymmetric band centered at  $639\text{ cm}^{-1}$ , whose structure markedly changes with increasing salt concentration. From 60:1 to 5:1, there is a broad, asymmetric band centered at  $642\text{ cm}^{-1}$ , with a shoulder at  $638\text{ cm}^{-1}$ . In the PEO:TbTf spectrum, there is a single band centered at  $637\text{ cm}^{-1}$  due to “free” ions. Thus, we can assign the shoulder at  $638\text{ cm}^{-1}$  in the PEO:LiTf system to “free” ions (or solvent-separated ion pairs). The broad band at  $642\text{ cm}^{-1}$ , which grows with increasing salt concentration, can be attributed to the  $(\text{Li}_2\text{Tf})^+$  species. In higher salt concentrations, another band appears at  $633\text{ cm}^{-1}$ . The two  $\nu(\text{C–S})$  factor group components at 320 and 312



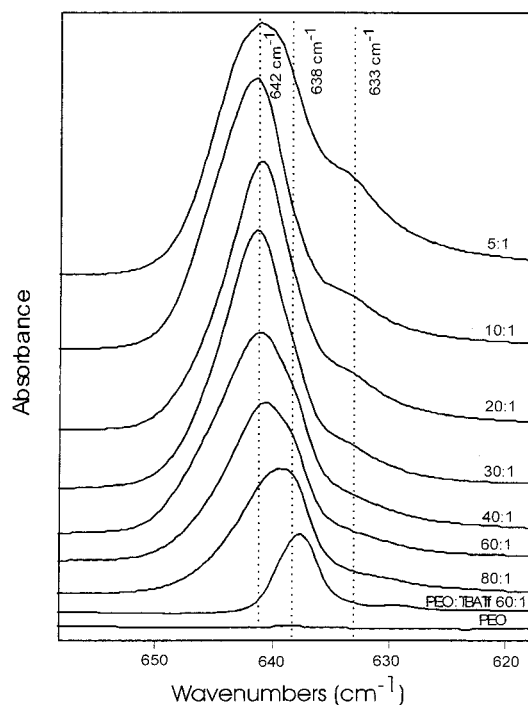


**Figure 4.** IR spectra of PEO, P(EO)<sub>60</sub>TBAF, and P(EO)<sub>n</sub>LiCF<sub>3</sub>SO<sub>3</sub> complexes ( $n = 80, 60, 40, 20, 10, 5$ ) in the  $\delta_s(\text{SO}_3)$  region. The spectra of the 30:1 through PEO compositions are shown on the same intensity scale. However, the spectra of the 20:1 through 5:1 compositions are shown on a different intensity scale for clarity of presentation.

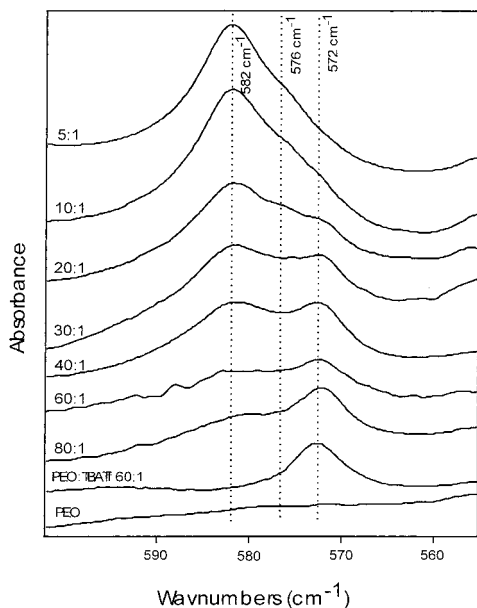


**Figure 5.** IR spectra of PEO, P(EO)<sub>60</sub>TBAF, and P(EO)<sub>n</sub>LiCF<sub>3</sub>SO<sub>3</sub> complexes ( $n = 80, 60, 40, 20, 10, 5$ ) in the  $\delta_{as}(\text{CF}_3)$  region. The spectra of the 40:1 through PEO compositions are shown on the same intensity scale. However, the spectra of the 30:1 through 5:1 compositions are shown on a different intensity scale for clarity of presentation.

$\text{cm}^{-1}$  could produce a combination band at  $632 \text{ cm}^{-1}$ ; alternatively, the  $633 \text{ cm}^{-1}$  band might be an overtone of the  $\nu(\text{C}-\text{S})$  band at  $320 \text{ cm}^{-1}$ .

Figure 5 shows the  $\delta_{as}(\text{CF}_3)$  mode as a function of salt concentration. Because this is a doubly degenerate mode for the isolated triflate ion, the bands split upon interaction with the cation(s), complicating band assignments. There are no pure PEO bands in this

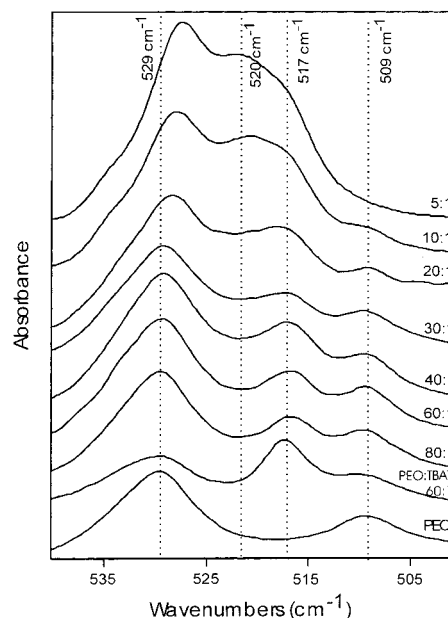


**Figure 6.** IR spectra of PEO, P(EO)<sub>60</sub>TBAF, and P(EO)<sub>n</sub>LiCF<sub>3</sub>SO<sub>3</sub> complexes ( $n = 80, 60, 40, 20, 10, 5$ ) in the  $\delta_{as}(\text{SO}_3)$  region. The intensity scale of the 5:1 spectra has been reduced for clarity of presentation.

region. We use the PEO:TBAF spectrum to identify the frequency of the band due to “free” ions at  $572 \text{ cm}^{-1}$  in both systems. With increasing salt concentration, two additional bands are observed at  $576$  and  $582 \text{ cm}^{-1}$ . The intensity of the band at  $582 \text{ cm}^{-1}$  increases with salt concentration and dominates the spectrum at higher salt concentrations. This behavior is similar to that of the  $(\text{Li}_2\text{Tf})^+$  band in the  $\delta_s(\text{CF}_3)$  region and is therefore attributed to the triple cation. The band at  $576 \text{ cm}^{-1}$  is attributed to contact ion pairs. It is interesting that we do not see evidence of splitting due to the breaking of degeneracy.

Spectra in the region of the  $\delta_{as}(\text{SO}_3)$  mode are shown in Figure 6. This region is particularly complicated, because there are both PEO and triflate bands present that are all dependent on salt concentration. In addition, the 2-fold degeneracy of this triflate mode is broken by cation–anion interactions. Pure PEO has bands at  $529$  and  $509 \text{ cm}^{-1}$  which have been assigned to CCO bending and  $\text{CH}_2$  rocking motions.<sup>22</sup> In PEO:TBAF and pure TBAF, we see a band at  $517 \text{ cm}^{-1}$ , which we attribute to “free” ions. Similarly, at low salt concentrations of the PEO:LiTf system, there is a band at  $517 \text{ cm}^{-1}$ , which we attribute to “free” ions. At high salt concentrations, a second feature at  $521 \text{ cm}^{-1}$  grows in intensity, which probably originates in the  $(\text{Li}_2\text{Tf})^+$  aggregate. Again, these band assignments are problematic as discussed above. The difficulties are exacerbated by our inability to assign a spectral feature in this region to the contact ion pair. In addition, we see that the PEO band at  $529 \text{ cm}^{-1}$  shifts to a lower frequency and the PEO band at  $509 \text{ cm}^{-1}$  disappears as the salt concentration increases.

Salt concentration-dependent spectra are shown in Figure 7 for the region from  $250$  to  $360 \text{ cm}^{-1}$ . Bands occurring at  $339$ ,  $347$ , and  $358 \text{ cm}^{-1}$  are attributed to the  $\rho(\text{SO}_3)$  vibrations of the various ionic species. Because this vibration is doubly degenerate in the “free” state, it is difficult to unambiguously assign each band to a particular species. The appearance of the two bands at  $339$  and  $347 \text{ cm}^{-1}$  in the 60:1 sample and the subsequent growth of their intensities suggests that

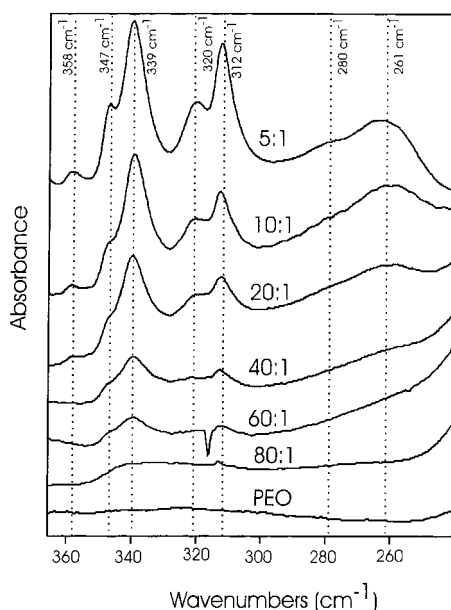


**Figure 7.** Far-IR spectra of PEO and  $\text{P(EO)}_n\text{LiCF}_3\text{SO}_3$  complexes ( $n = 100, 80, 60, 40, 20, 10, 5$ ) in the  $\rho(\text{SO}_3)$  and  $\nu(\text{C}-\text{S})$  regions. The intensity scale of the 5:1 spectra has been reduced for clarity of presentation.

these may be related to the two components expected from the breaking of  $\rho(\text{SO}_3)$  degeneracy in the  $\text{P(EO)}_3\text{-LiTf}$  compound. The weak band at  $358\text{ cm}^{-1}$  may be a factor group component from this same vibration.

The two bands at  $312$  and  $320\text{ cm}^{-1}$  are assigned to two factor group components of the  $\text{C}-\text{S}$  stretching vibration,  $\nu(\text{C}-\text{S})$ . This assignment is based on the observation that the relative intensities of the two bands are independent of salt concentration. If these two bands resulted from different ionic species such as an ion pair and the triple cation, one would expect the relative intensities to alter dramatically, similar to the changes in the  $\delta_s(\text{CF}_3)$  modes that occurred as the proportions of the species changed with total salt concentration.

At high salt concentrations, there is also a broad band at  $261\text{ cm}^{-1}$  and a shoulder at  $280\text{ cm}^{-1}$ . These features grow with increasing salt concentration in a manner similar to that observed in the  $\delta_s(\text{CF}_3)$  regions. However it is difficult to assign these bands with any degree of confidence.

#### 4. Summary

The comparative analysis of the integrated band intensities clearly demonstrates that the two absorption bands from the  $\nu(\text{Li}-\text{O})$  modes are each associated with the vibrations of all cations in all cationic environments. This conclusion is in contrast with the more intuitive (but incorrect) interpretation that two distinct bands arise from lithium ions in two distinct vibrational potential energy environments.

The frequencies and band intensities of a number of low-frequency triflate ion intramolecular vibrations are reported as a function of salt concentration. Assignments of the band components within each spectral region were aided by comparison with the salt concentration dependence of the well-characterized triflate  $\delta_s(\text{CF}_3)$  mode. In most cases, identification of the "free" ion frequency in each spectral region was made possible

by comparison with the spectrum of  $\text{TbaTf}$ . The bulky  $\text{Tba}$  cation precludes any significant degree of ionic association; hence, the bands present are due to "free" ions. The  $\delta_s(\text{SO}_3)$  and  $\delta_{as}(\text{CF}_3)$  regions contained both "free" ion bands and  $(\text{Li}_2\text{Tf})^+$  bands that could easily be identified. "Free" ions could also be easily seen in the  $\delta_{as}(\text{SO}_3)$  region; however, the identification of the  $(\text{Li}_2\text{Tf})^+$  species was problematic. It was not possible to assign distinct ionic species to bands in the  $\rho(\text{SO}_3)$  and  $\nu(\text{C}-\text{S})$  regions. This difficulty may arise in part because of the low frequencies of these modes and extensive mode mixing.

The broad band at  $261\text{ cm}^{-1}$  and the shoulder at  $280\text{ cm}^{-1}$  observed at high salt concentrations remain unassigned and, consequently, the object of future studies. We will also focus on PEO modes in the very low-frequency region. Such modes may reflect the effects of  $\text{LiTf}$  addition on vibrations involving the larger subunits of the polymer chain undergoing coupled torsional and bending motions. In that case, an investigation of these modes may lead to insight into the nature of polymer segmental motion.

**Acknowledgment.** We thank Chris Rhodes and Fred McKenna for useful discussions. This work was supported by NSF Cooperative Agreement EPS 9720651 and a grant from the Research Corporation, RA0306.

#### References and Notes

- (1) Fenton, D. E.; Parker, J. M.; Wright, P. V. *Polymer* **1973**, *14*, 589.
- (2) Armand, M. B.; Chabagno, J. M.; Duclot, M. J. In *Proceedings of the International Conference on Fast Ion Transport in Solids*; Vashista, P., Mundy, J. N., Shenoy, G. K., Eds.; Elsevier, North Holland: New York, 1979; p 131.
- (3) Scrosati, B. In *Modern Batteries: An Introduction to Electrochemical Power Sources*; Vincent, C. A., Scrosati, B., Eds.; John Wiley & Sons: New York, 1997.
- (4) Berthier, C.; Gorecki, W.; Minier, M.; Armand, M. B.; Chabagno, J. M.; Rigaud, P. *Solid State Ionics* **1983**, *11*, 91.
- (5) MacCallum, J. R.; Vincent, C. A. In *Polymer Electrolyte Reviews*; MacCallum, J. R., Vincent, C. A., Eds.; Elsevier: New York, 1987; Vol. 1.
- (6) Ratner, M. A.; Nitzan, A. *Faraday Discuss. Chem. Soc.* **1989**, *88*, 19.
- (7) Papke, B. L.; Ratner, M. A.; Shriver, D. F. *J. Phys. Chem. Solids* **1981**, *42*, 493.
- (8) Schantz, S.; Sandahl, J.; Börjesson, L.; Torell, L. M.; Stevens, J. R. *Solid State Ionics* **1988**, *28-30*, 1047.
- (9) Schantz, S.; Torell, L. M.; Stevens, J. R. *J. Chem. Phys.* **1991**, *94*, 6862.
- (10) Frech, R.; Huang, W. *Solid State Ionics* **1994**, *72*, 103.
- (11) Frech, R.; Huang, W. *Macromolecules* **1995**, *28*, 1246.
- (12) Petersen, G.; Jacobsson, P.; Torell, L. M. *Electrochim. Acta* **1992**, *37*, 1495.
- (13) Huang, W.; Frech, R. *Polymer* **1994**, *35*, 235.
- (14) Frech, R.; Huang, W. *Solid State Ionics* **1993**, *66*, 183.
- (15) Papke, B. L.; Ratner, M. A.; Shriver, D. F. *J. Electrochem. Soc.* **1982**, *129*, 1434.
- (16) Robitaille, C. D.; Fauteux, D. *J. Electrochem. Soc.* **1986**, *133*, 315.
- (17) Vallee, A.; Besner, S.; Prud'homme, J. *Electrochim. Acta* **1992**, *37*, 1579.
- (18) Frech, R.; Chintapalli, S.; Bruce, P. G.; Vincent, C. A. *Chem. Commun.* **1997**, 157.
- (19) Frech, R. *Macromolecules* **2000**, *33*, 9432.
- (20) Lightfoot, P.; Mehta, M. A.; Bruce, P. G. *Science* **1993**, *262*, 883.
- (21) Frech, R.; Huang, W. *J. Solution Chem.* **1994**, *23*, 469.
- (22) Miyazawa, H. M. A. T. *Bull. Chem. Soc. Jpn.* **1968**, *41*, 1798.